

UC Irvine

UC Irvine Previously Published Works

Title

Geometry and flow influences on jet mixing in a cylindrical duct

Permalink

<https://escholarship.org/uc/item/7rm3355n>

Journal

Journal of Propulsion and Power, 11(3)

ISSN

0748-4658

Authors

Hatch, MS
Sowa, WA
Samulersen, GS
[et al.](#)

Publication Date

1995-05-01

DOI

10.2514/3.23857

Copyright Information

This work is made available under the terms of a Creative Commons Attribution License, available at <https://creativecommons.org/licenses/by/4.0/>

Peer reviewed

Geometry and Flow Influences on Jet Mixing in a Cylindrical Duct

M. S. Hatch,* W. A. Sowa†, and G. S. Samuelsen‡
University of California, Irvine, Irvine, California 92717
and
J. D. Holdeman§
NASA Lewis Research Center, Cleveland, Ohio 44135

To examine the mixing characteristics of jets in an axisymmetric can geometry, temperature measurements were obtained downstream of a row of cold jets injected into a heated cross stream. Parametric, nonreacting experiments were conducted to determine the influence of geometry and flow variations on mixing patterns in a cylindrical configuration. Results show that jet-to-mainstream momentum-flux ratio and orifice geometry significantly impact the mixing characteristics of jets in a can geometry. For a fixed number of orifices, the coupling between momentum-flux ratio and injector geometry determines 1) the degree of jet penetration at the injection plane and 2) the extent of circumferential mixing downstream of the injection plane. The results also show that, at a fixed momentum-flux ratio, jet penetration decreases with 1) an increase in slanted slot aspect ratio and 2) an increase in the angle of the slots with respect to the mainstream direction.

Nomenclature

DR	= jet-to-mainstream density ratio
ϕ	= orifice angle with respect to mainstream
f	= mixture fraction
J	= jet-to-mainstream momentum flux ratio
MOD1	= eight-hole baseline geometry
MOD2	= 8:1 aspect ratio slanted slots, $\phi = 45$ deg
MOD3	= 4:1 aspect ratio slanted slots, $\phi = 0$ deg
MOD4	= 4:1 aspect ratio slanted slots, $\phi = 22.5$ deg
MOD5	= 4:1 aspect ratio slanted slots, $\phi = 45$ deg
MOD6	= 4:1 aspect ratio slanted slots, $\phi = 67.5$ deg
MOD7	= 4:1 aspect ratio slanted slots, $\phi = 90$ deg
MR	= jet-to-mainstream mass ratio

Introduction

MIXING of jets in a confined crossflow has a variety of practical applications and has motivated a number of studies over the past decades. In a gas turbine combustor, e.g., mixing of relatively cold air jets is important in the dilution zone where the products of combustion are mixed with air to reduce the temperatures to levels acceptable for the turbine blade material. Mixing of jets in a crossflow is also important in applications such as discharge of effluents in water, and in transition from hover to cruise of V/STOL aircraft.

To meet the air quality standards affecting gas turbines, low emissions combustors are being developed.¹ One of the

promising low NO_x combustor concepts is the rich-burn/quick-mix/lean-burn (RQL) combustor.² The RQL developmental effort poses new challenges in jet mixing in a confined crossflow.^{1,2} More specifically, the range of jet-to-mainstream mass flow ratios encountered in the quick-mix region of a RQL combustor differ significantly from those of a conventional combustor dilution zone.^{3–5}

Most of the previous research of jets in a crossflow has been performed in rectangular geometries. Examples of these studies are provided in Table 1 and are summarized elsewhere.⁶ The influence of orifice geometry and spacing, jet-to-mainstream momentum-flux ratio J , and density ratio have been documented for single- and double-sided injection (e.g., Ref. 6). These studies have identified J and orifice spacing as the most significant parameters influencing the mixing pattern.

Experiment

A series of parametric experiments were conducted in this study to determine the influence of J and orifice configuration on mixing of jets in a can geometry. The parametric experiments investigated a range of J values, including 25, 52, and 80. A jet-to-mainstream mass ratio of 2.2 was maintained at each tested J value. An area discharge coefficient of 0.80 was assumed in designing the orifices.

The modules tested in the parametric studies were fabricated from a 3-in.- (76-mm-) i.d., 0.125-in.- (3.18-mm-) thick Plexiglas® tubing. Plexiglas was selected for its optical quality and ease of fabrication. For each J value, configurations with eight, equally spaced orifices were evaluated. The geometries included: 1) round holes (module 1); 2) 4:1 aspect ratio slots oriented at various angles with respect to the mainstream flow direction: 0 deg (module 3), 22.5 deg (module 4), 45 deg (module 5) 67.5 deg (module 6), and 90 deg (module 7); and 3) 8:1 aspect ratio slots oriented at 45 deg (module 2).

The modules were 6.5 in. (165 mm) long, with the center of the orifice row placed at one radius from the edge. The orifice area for each module at the design J value was kept constant. As a result, the dimensions of a given orifice varied as a function of J . A representative module is shown in Fig. 1. (All modules are presented in Ref. 7.) While the leading edge of each orifice was fixed at the same axial location ($z/R = 0.0$), the axial extent of jet mass addition varied according to orifice size and, in the case of the slots, slot angle

Presented as Paper 92-0773 at the AIAA 30th Aerospace Sciences Meeting and Exhibit, Reno, NV, Jan. 6–9, 1992; received March 18, 1993; revision received June 2, 1994; accepted for publication July 14, 1994. Copyright © 1992 by the American Institute of Aeronautics and Astronautics, Inc. No copyright is asserted in the United States under Title 17, U.S. Code. The U.S. Government has a royalty-free license to exercise all rights under the copyright claimed herein for Governmental purposes. All other rights are reserved by the copyright owner.

*Graduate Researcher, UCI Combustion Laboratory. Student Member AIAA.

†Associate Director, UCI Combustion Laboratory. Member AIAA.

‡Professor, Director, UCI Combustion Laboratory. Associate Fellow AIAA.

§Senior Research Engineer. Associate Fellow AIAA.

Table I Summary of selected jet mixing studies

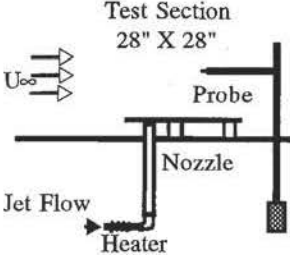
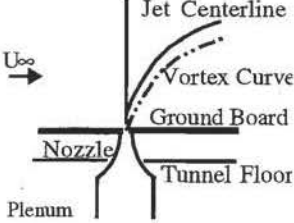
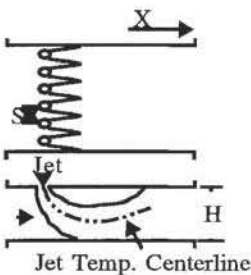
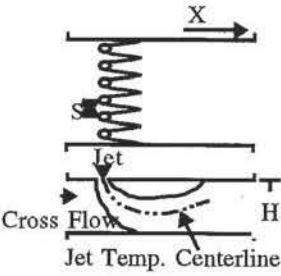
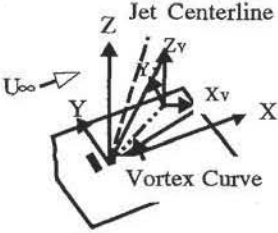
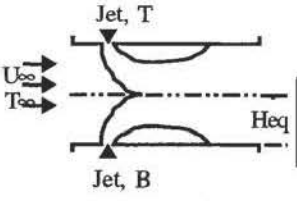
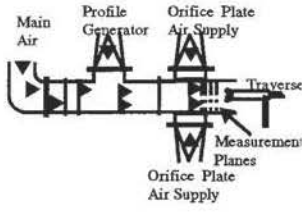
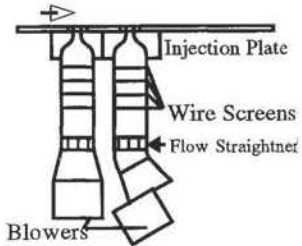
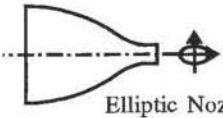
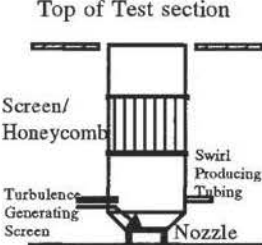
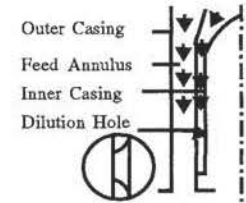
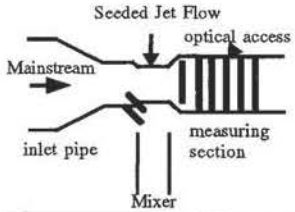
Reference	Configuration	Test parameters	Measurements	Diagnostics	Major conclusions
8	 <p>Test Section 28" X 28"</p> <p>Probe</p> <p>Nozzle</p> <p>Jet Flow</p> <p>Heater</p> <p>U_{∞}</p>	J : 15–60 U_z : 20–30 fps Re : 2800–4200 T_{jet} : 75–400 F	Flow visualization Velocity Turbulent intensity Temperature	Smoke Photograph Hot wire Thermocouple	Momentum-flux ratio determines the jet trajectory. Turbulent intensity grows with momentum-flux ratio. Temperature profile and density ratio weakly related. Downstream temperature and velocity distribution is affected by vortex motion.
9	 <p>Jet Centerline</p> <p>Vortex Curve</p> <p>Ground Board</p> <p>Nozzle</p> <p>Tunnel Floor</p> <p>Plenum</p> <p>U_{∞}</p>	VR : 3–10 U_z : 100–175 fps T_{jet} : 75–400 F	Velocity field	Yaw pitch Probe	Developed two models of contrarotating vortices. The pair of vortices is the dominant flowfield feature. The vortex pair is formed close to the injection point. Vortices initial strength is proportional to nozzle diameter and jet speed
10	 <p>X</p> <p>Jet</p> <p>H</p> <p>Jet Temp. Centerline</p> <p>U_{∞}</p>	$13 \leq J \leq 63$ $0.1 \leq MR \leq 0.6$ $2.5 \leq VR \leq 5.3$	Temperature Pressure	Thermocouple Not reported	Developed model to predict temperature downstream of one row of closely spaced holes injected into a hot confined crossflow. The model predicted well the measured flowfield for parameters representative of current GT combustors.
11	 <p>X</p> <p>Jet</p> <p>H</p> <p>Jet Temp. Centerline</p> <p>Cross Flow</p> <p>U_{∞}</p>	$13 \leq J \leq 63$ $0.1 \leq MR \leq 0.6$ $2.5 \leq VR \leq 5.3$	Temperature Pressure	Thermocouple Not reported	Developed an empirical model to predict mixing of one row of jets injected into a hot crossflow. The model predicted well the measured flowfield. Momentum-flux ratio was most important factor influencing mixing.
12	 <p>Jet Centerline</p> <p>Vortex Curve</p> <p>U_{∞}</p> <p>Z</p> <p>Y</p> <p>X</p> <p>X_v</p> <p>Z_v</p>	Slots: 4:1 Aspect ratio, Blunt, streamwise Velocity ratio: 4, 8, 10 Jet angle: 15–90 deg	Pressure Velocity Flow angularity	Yaw pitch Probes	Penetration and vortex strength—blunt jets lowest. Nominal properties of streamwise jets are similar to those of circular jets. Rectangular jets decay faster than round jets due to increased viscous effects on larger perimeter.
13	 <p>Jet, T</p> <p>Jet, B</p> <p>Heq</p> <p>U_{∞}</p> <p>T_{∞}</p>	JT : 9–58 JB : 24–60 U_z : 14–18 m/s T_{jet} : 309–319 K T_z : 430–558 K	Temperature Pressure Velocity	NiCr-Ni TC Pressure probe Not reported	One-sided wall injection correlations can be used for opposite-wall jet injection at low momentum-flux ratios. Modified correlations give better agreement at higher momentum-flux ratios.

Table 1 (Continued) Summary of selected jet mixing studies

Reference	Configuration	Test parameters	Measurements	Diagnostics	Major conclusions
14		$H_0/D: 4, 8$ $S/D: 2, 4$ $DR: 0.75, 2.2$	Temperature Pressure	TC Total and static Pressure probes	Mixing impacted by wall convergence and by density ratio, a second-order effect. Optimum orifice spacing for opposed in-line jets is half of the optimum value for the single-sided case. For staggered jets the optimum value is twice the one of single-side injection.
15		$VR = 2$ Single jet Tandem jets	Mean velocities Reynolds stresses	Hot wire	Similarity observed for the cross sections of single and tandem jets. The transverse velocity profiles were different from axial and vertical profiles. Initial conditions set the jet trajectory.
16		$V_j = 21.9 \text{ m/s}$ Aspect ratio: 2:1	Velocities	Hot wire	Mass entrainment by a 2:1 aspect ratio elliptic jet is significantly higher than that of a round hole.
17		$VR: 2.2, 4, 8$ Turbulence: $3\%, >10\%$ Swirl: $40\%, 58\%$	Pressure Velocity Turbulence	Yawhead probe Hot wire X-wire probe	Swirl and high turbulence reduce penetration and decrease negative pressure surface area. Swirl produces asymmetry in pressure distribution, especially for low velocity ratios, and high swirl ratios.
18		$13 \leq J \leq 63$ $0.1 \leq MR \leq 0.6$ $2.5 \leq VR \leq 5.3$	Temperature Pressure	Thermocouple Not reported	Developed an empirical model to predict mixing of one row of jets injected into a hot cross-flow. The model predicted well the measured flowfield. Momentum-flux ratio was most important factor influencing mixing.
5		$4:1$ and $8:1$ AR Slots and round holes Slot angle: 45 deg $J: 5, 18, 78$	Seed Concentration	Mie scattering Planar digital Imaging	Slanted slots are better mixers above a certain J . Mixing decreases at increased density ratios. Mixedness is independent of mass flow rate.

and slot aspect ratio as well. For reference, the axial location of the trailing edge and blockage are presented in Table 2. The former is expressed as the ratio of the axial projection of the orifice to the radius of the mixing module, and the latter is defined as the ratio of the circumferential projection of the orifice to the spacing between orifice centers.

Mixing was examined by measuring the local mean temperature throughout the module. The mainstream flow entering the module was heated to the highest temperature (212°F) compatible with the upper temperature limits of Plexiglas. Jets were introduced at room temperature.

The operating conditions are presented in Table 3. Reference velocity, defined as the velocity at the inlet to the mixing section and calculated based on the mainstream temperature and pressure, was 34.5 fps (10.5 m/s). The actual discharge coefficient, and momentum-flux ratio for each case was determined by measuring the jet pressure drop.

A 12-in.-long, 0.125-in. type K thermocouple was used to measure the temperatures. Temperature was measured at 50 points in a quarter sector of the modules, for five planes downstream of the orifices. Figures 2a and 2b show the measurement points and the axial planes. A 90-deg sector was

Table 2 Axial location of orifice trailing edge and orifice blockage

Module	Hole/slot	Aspect ratio	Angle	Axial projection/radius of mixing module			Circumferential projection/spacing between orifice centers		
				$J = 25$	$J = 52$	$J = 80$	$J = 25$	$J = 52$	$J = 80$
1	Hole	—	—	0.5	0.42	0.37	0.64	0.53	0.48
2	Slot	8:1	45	0.89	0.74	0.66	1.19	0.99	0.89
3	Slot	4:1	0	0.90	0.75	0.67	0.29	0.24	0.21
4	Slot	4:1	22.5	0.83	0.69	0.62	0.62	0.51	0.46
5	Slot	4:1	45	0.63	0.53	0.48	0.90	0.74	0.67
6	Slot	4:1	67.5	—	0.28	0.26	—	0.90	0.81
7	Slot	4:1	90	—	—	0.17	—	—	0.86

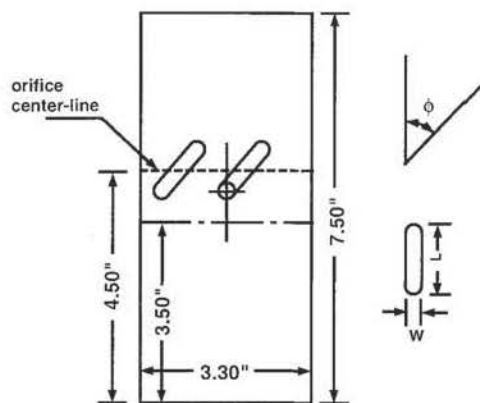
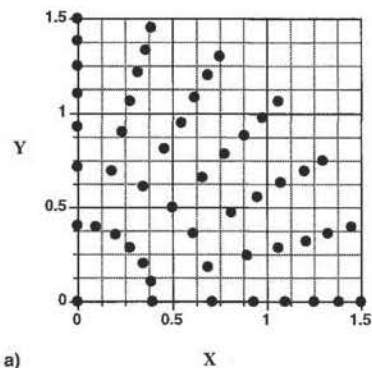


Fig. 1 Mixing module dimensions.



a)

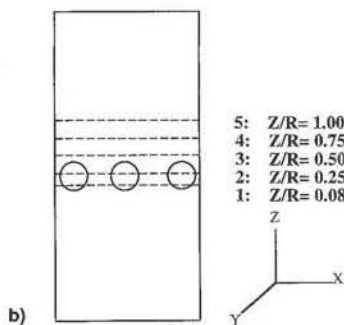


Fig. 2 Measurement points and planes.

selected to examine the interaction of the adjacent jets and the asymmetries of the flowfield. The five planes examined in this study were located between $z/R = 0.08$, and $z/R = 1.0$, where Z was measured from the leading edge of the orifices.

Experimental Facility

The test facility that is located at the UCI Combustion Laboratory and is shown schematically in Fig. 3 featured house

Table 3 Experimental operating conditions

T_{main} , °F	T_{jet} , °F	P , psia	V_{main} , fps	M_{main} , pps	MR	DR
212	74	14.7	34.5	0.10	2.2	1.26

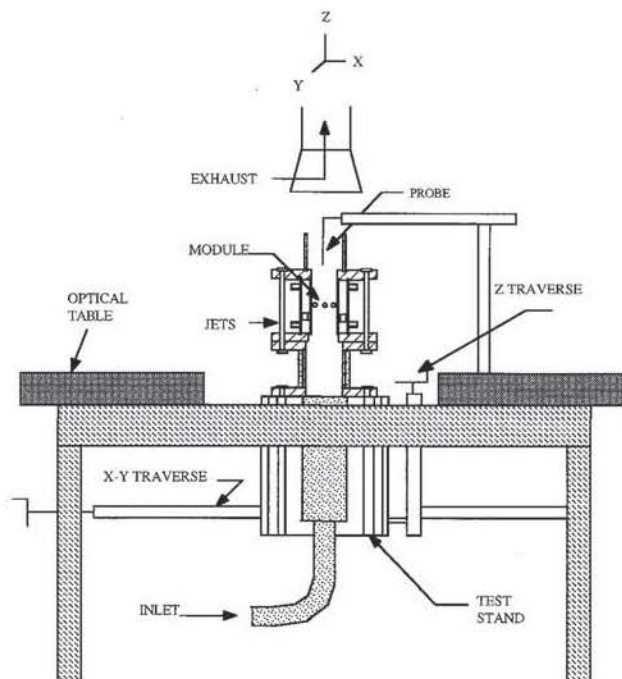


Fig. 3 Schematic of the test facility.

air that was filtered and regulated before branching into two isolated main and jet circuits. The jet circuit incorporated four independently metered flow legs. The main circuit consisted of a coarse and a fine leg that provided a total of 150 standard cubic feet per second (SCFM) for the mainstream flow. Each leg was regulated independently to eliminate the effects of pressure fluctuations. All circuits were metered by sonic venturies. The mainstream air was heated to 212°F by a 20-kW air preheater (Watlow, P/N 86036-2). The outlet temperature was controlled by a Watlow heater controller (series 800).

The mainstream air, after being metered and heated, passed through flexible tubing into a 2-in. insulated carbon steel pipe immediately upstream of the mixing module. A combination honeycomb/screen in the pipe provided uniform flow to the mixing module. The flexible tubing upstream of the pipe allowed manual traversing of the experiment in the X , Y , and Z directions. A Mitutoya model PM-331 digital traverse read-out was used to read the coordinates.

The 3-in. mixing module used in the parametric phase was positioned inside a concentric Pyrex® manifold (see Fig. 3). The jet manifold incorporated four openings on top and four

on the bottom, each 90 deg apart. Four discrete jets were supplied to the manifold through the bottom openings. Two of the openings on the top were used to measure the manifold temperature and pressure, and the other two were blocked. Each jet circuit was metered individually and installed to provide symmetric flow conditions at the inlet to the manifold. Honeycomb was installed in the jet plenum upstream of the orifices to provide uniform flow through the mixing module.

Analysis

To compare the mixing characteristics of different modules, the temperature measurements were normalized by defining the mixture fraction f at each point in the plane:

$$f = \frac{T_{\text{measured}} - T_{\text{jet}}}{T_{\text{main}} - T_{\text{jet}}} \quad (1)$$

A value of $f = 1.0$ corresponds to the mainstream temperature, whereas $f = 0$ indicates the presence of the pure jet flow. Complete mixing occurs when f approaches the equilibrium value that is nearly equal to the ratio of the upstream flow to the total flow. Note that $f = 1 - \theta$, where θ appears in previous studies.⁶

To quantify the mixing effectiveness of each module configuration, an area-weighted standard deviation parameter ("mixture uniformity") was defined at each z/R plane:

$$\text{mixture uniformity} = \sqrt{\frac{1}{A} \sum_{i=1}^n a_i (f_i - f_{\text{equil}})^2} \quad (2)$$

where $A = \sum a_i$, f_i is the mixture fraction calculated for each node, and f_{equil} is the equilibrium mixture fraction, defined as

$$f_{\text{equil}} = \frac{T_{\text{equil}} - T_{\text{jet}}}{T_{\text{main}} - T_{\text{jet}}} \quad (3)$$

Complete mixing is achieved when the mixture uniformity parameter across a given plane reaches zero.

Results and Discussion

This section presents the mixing characteristics for the baseline geometry (module 1), and the 8:1 and 4:1 slanted slots configurations (module 2 and module 5) as a function of momentum-flux ratio. In addition, the effects of slot aspect ratio and orientation on mixing pattern are discussed. From an overall-mixing standpoint, an optimum mixer is defined as one that produces a uniformly mixed flowfield, without a persistent unmixed core or unmixed circumferential regions by the $z/R = 1.0$ plane. In the contour plots presented, the center of the jets are located at 22.5 and 67.5 deg, relative to the measurement plane. For slanted slots, the jets angle counterclockwise as one moves upstream.

Module 1—Baseline Geometry (Holes)

Three baseline geometries were tested as part of the parametric experiments. Figures 4 and 5 present the mixture fraction variations between planes $z/R = 0.0$ to $z/R = 1.0$ for the momentum-flux ratio range endpoints: $J = 25$, and 80 (cases $J25MOD1$ and $J80MOD1$). The actual J is shown in the figure caption.

A comparison of the mixture fraction distribution at the first axial location ($z/R = 0.0$) shows a decrease in f at the center, with increasing momentum-flux ratio. For $J = 25$ ($J25MOD1$), f is in the range of 0.8–0.9 at the core of the module, indicating the penetration of some jet fluid to the center. For $J = 80$ ($J80MOD1$), the mixture fraction values at the center are in the range 0.2–0.3. These f values are at or below the totally mixed value of $f(f_{\text{equil}} = 0.31)$ indicating overpenetration to the center.

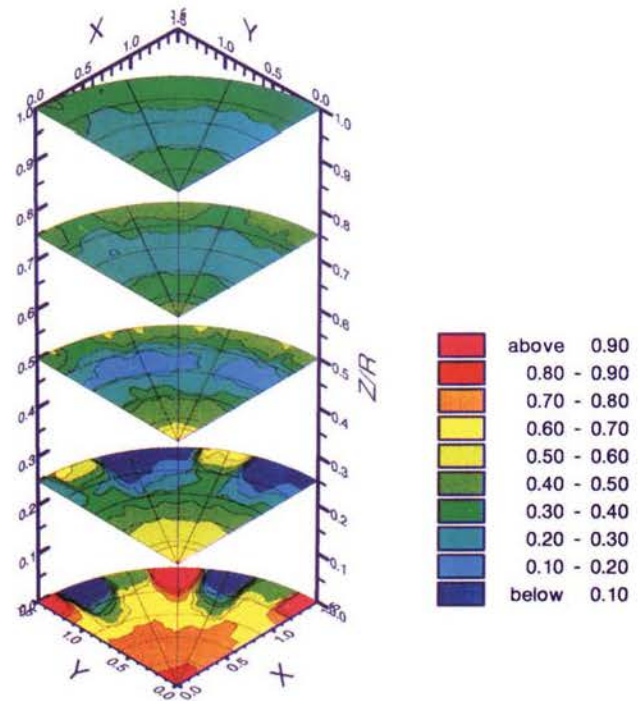


Fig. 4 Mixture fraction, $J25MOD1$, baseline eight-hole, $J = 26.7$.

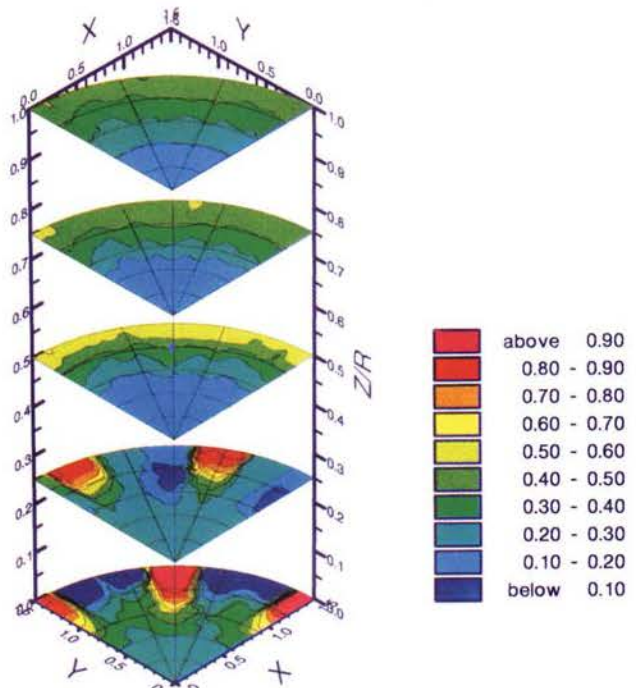


Fig. 5 Mixture fraction, $J80MOD1$, baseline eight-hole, $J = 84.2$.

At the jet injection locations for $J = 25$ ($J25MOD1$), f decreases monotonically in the radial direction, with the highest concentration of mainstream fluid on the duct centerline ($R = 0.0$), and lowest at the walls ($R = 1.5$). The monotonic variation of f indicates that no backflow exists for this configuration. The radial variation of f at $z/R = 0.0$ for $J = 80$ ($J80MOD1$), on the other hand, is nonmonotonic. For the $J = 80$ module at the injection location, f is relatively low at $R = 0.0$, increases as R is increased, and approaches zero at the jet inlet. This nonmonotonic variation of f indicates backflow and overpenetration of jets for these configurations.

Overpenetration of jets is evident at the downstream axial locations for $J = 80$ ($J80MOD1$) by the high f near the wall.

At $z/R = 1.0$, the $J = 80$ module ($J80MOD1$) shows low f values at the center, and an unmixed region along the wall, whereas $J = 25$ ($J25MOD1$) shows a more uniformly mixed flowfield. The degradation in mixing for $J = 80$ ($J80MOD1$), occurs because the increased jet penetration to the module center directs a larger portion of the jet flow to the core, thus decreasing the circumferential mixing along the walls. In an axis-symmetric can geometry, where the majority of the mass is concentrated along the walls, good circumferential mixing is important in obtaining a well-mixed flowfield. Therefore, according to the definition presented earlier, the round holes at $J = 25$ ($J25MOD1$) display closer to optimum mixing than the $J = 80$ case at $z/R = 1.0$. Following the methodology of Eq. (6) found in Holdeman,⁶ the optimum momentum-flux ratio for this eight-orifice case would be just over 20.

Figure 6 compares the mixture uniformity parameter for all of the baseline modules tested as a function of momentum flux ratio. This plot confirms the qualitative observation that the increase in the momentum-flux ratio improves mixing at the initial planes, but degrades the overall mixing downstream of the injection plane.

Module 2—(8:1 Slots; 45 Deg)

Three 8:1 aspect ratio geometries were examined during the parametric studies. Figures 7 and 8 present the mixture

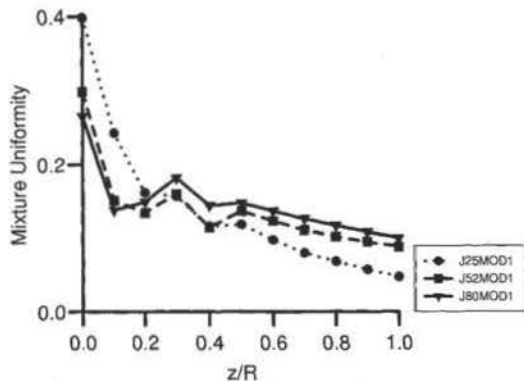


Fig. 6 Mixture uniformity for baseline modules.

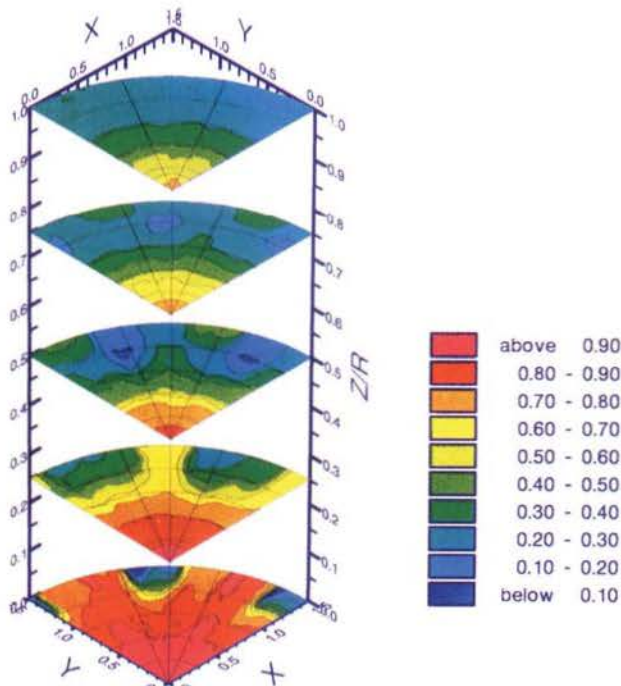


Fig. 7 Mixture fraction, $J25MOD2$, 8:1 aspect ratio slanted slots, angle = 45 deg, $J = 28.1$.

fraction distribution for the momentum-flux ratio range endpoints: $J = 25$ and 80 (cases $J25MOD2$ and $J80MOD2$).

The first axial location ($z/R = 0.0$) examined for the $J = 25$ module shows a large region at $f > 0.9$, indicating very small or no jet penetration to the center. For this configuration, the relatively unmixed core persists with increasing z/R , and is present at the last axial location of $z/R = 1.0$. This configuration represents an underpenetrated case.

The first indication of jet penetration to the center for the three 8:1 aspect ratio modules tested is observed at the $z/R = 0.0$ plane of the $J = 80$ ($J80MOD2$) module. The mixture fraction value at the core of this plane ranges between 0.8–0.9 indicating that a portion of jet fluid is mixed with the mainstream. At the $z/R = 1.0$ plane, the main portion of the flow is close to the equilibrium value, while a slightly larger f is seen at the center. The presence of the slightly warmer core shows that this configuration is still slightly underpenetrated. Mixing characteristics of this module are similar to those at $J = 25$ ($J25MOD1$).

Figure 9 compares the mixture uniformity parameter for the 8:1 aspect ratio geometries. At the first axial location, the $J = 25$ module ($J25MOD2$) produces degraded mixing due

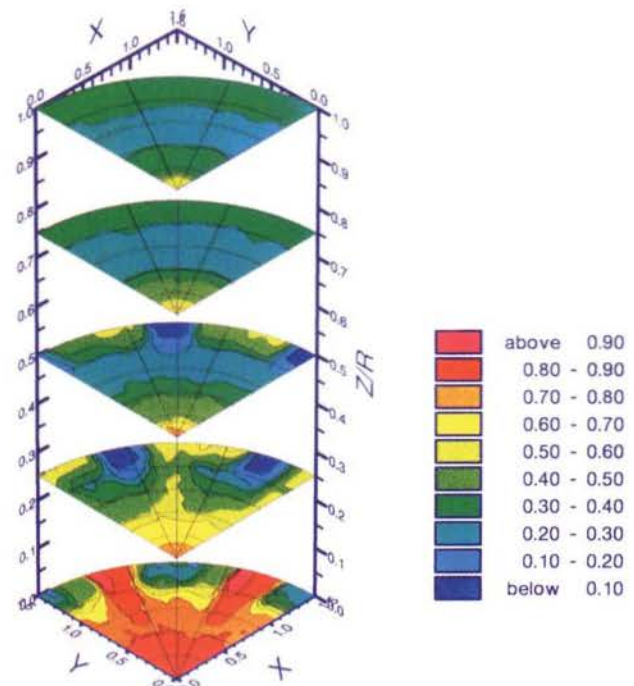


Fig. 8 Mixture fraction, $J80MOD2$, 8:1 aspect ratio slanted slots, angle = 45 deg, $J = 88.5$.

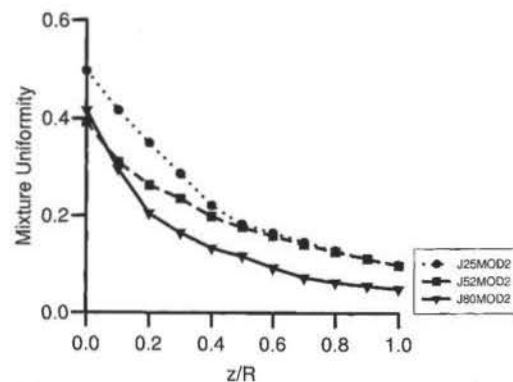


Fig. 9 Mixture uniformity for 8:1 aspect ratio slanted slots, angle = 45 deg.

to underpenetration. For increased J values, mixing at the first axial location is improved. The mixing performances for $J = 52$ ($J52MOD2$), and $J = 80$ ($J80MOD2$) are similar at the initial axial planes. Beyond $z/R = 0.2$, however, $J = 80$ ($J80MOD2$) clearly produces the better mixing.

Module 5—(4:1 Slots; 45 Deg)

Figures 10 and 11 present the mixture fraction distribution for the momentum flux ratio range endpoints: $J = 25$ and 80 (cases $J25MOD5$ and $J80MOD5$). The first axial location for the $J = 25$ module (at $z/R = 0.0$) shows a relatively large central region with mixture fraction values in the range of 0.8–0.9. This f value is less than unity, indicating slight jet penetration and mixing at the center of the module. Compared to the round hole jets ($J25MOD1$), the region of near unity values of f is larger. The jet penetration for the round hole jets is stronger at this J value, therefore, the high mixture fraction region is smaller. As described previously, the 8:1 aspect ratio module at $J = 25$ ($J25MOD2$) represents a case of underpenetration with central f values above 0.9. At downstream locations, the $J = 25$ module ($J25MOD5$) produces a relatively well-mixed flowfield with no indication of unmixed walls. At $z/R = 1.0$, however, a slightly unmixed core is observed.

As J is increased, the penetration to the center is enhanced and the mixture fraction values at the core of the module at initial axial locations decrease. At $J = 80$ ($J80MOD5$), a relatively low f value region is seen at the first axial location. At downstream locations, a cool center and relatively unmixed regions along the walls are produced. At this momentum-flux ratio as well as at $J = 52$ ($J52MOD5$), the jets overpenetrate, a condition that is not desirable from an overall mixing standpoint.

Figure 12 compares the mixture uniformity parameter for the three 4:1 aspect ratio geometries. The trend is very similar to that described for the baseline modules. At initial planes, the higher the momentum-flux ratio, the better the mixture uniformity. At downstream locations, the J value with the most initial overpenetration (80), is the poorer mixer due to degradation of circumferential mixing ($J80MOD5$).

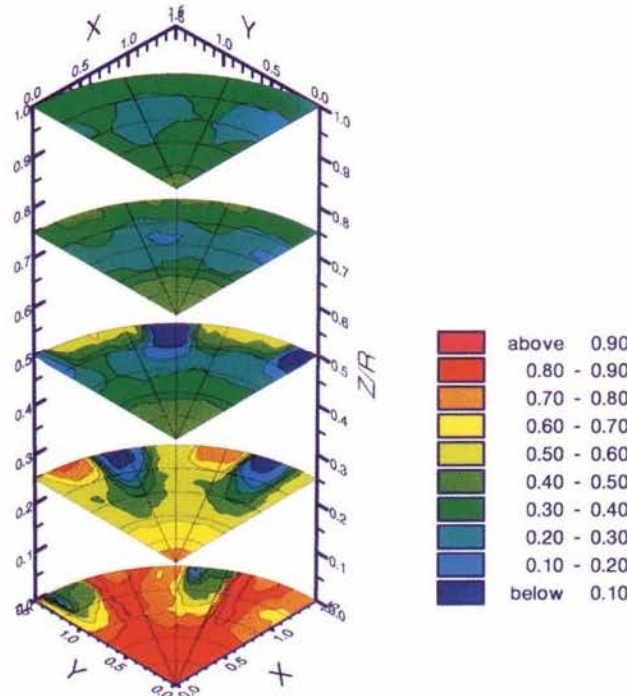


Fig. 10 Mixture fraction, $J25MOD5$, 4:1 aspect ratio slanted slots, angle = 45 deg, $J = 30.5$.

Effect of Slot Aspect Ratio and Angle on Mixing Pattern

The slot aspect ratio affects 1) the amount of jet mass injected per unit length and 2) the axial extent over which the mass is injected.

For a given momentum-flux ratio and number of orifices, the smaller aspect ratio slots penetrate further into the cross stream. The larger aspect ratio slots on the other hand, produce a stronger swirl component that enhances the circumferential mixing. Figure 13 compares the mixture uniformity parameter for the 8:1 and 4:1 aspect ratio slots. At the lower and intermediate J values, the 4:1 aspect ratio geometry is a better mixer at all axial locations. At the highest J value tested, however, the 8:1 aspect ratio behaves as the better mixing geometry beyond $z/R = 0.5$. This is because of the overpenetration of jets at $J = 80$ ($J80MOD5$), which improves mixing at the initial planes, but produces unmixed regions along the walls at downstream axial locations. As the slot angle is changed, the J value at which one mixer demonstrates more desirable mixing characteristics than the other can change also.

The slot angle affects 1) the axial length over which jet mass is injected and 2) the “blockage” that the jets present to the

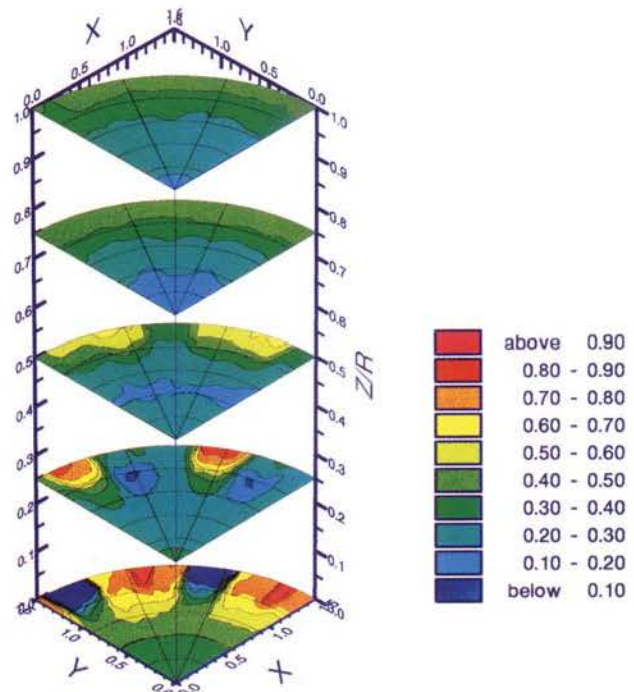


Fig. 11 Mixture fraction, $J80MOD5$, 4:1 aspect ratio slanted slots, angle = 45 deg, $J = 93.0$.

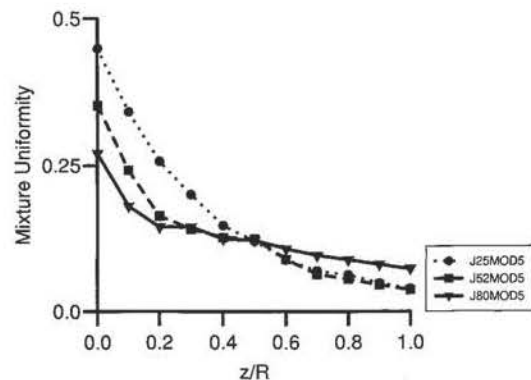


Fig. 12 Mixture uniformity for 4:1 aspect ratio slanted slots, angle = 45 deg.

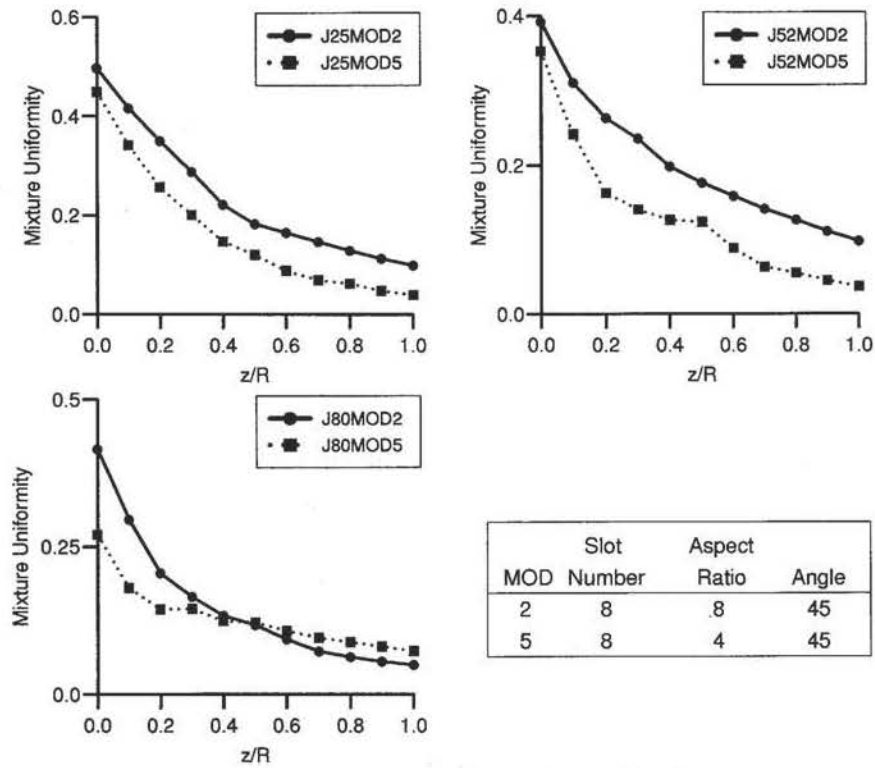


Fig. 13 Effect of slot aspect ratio on mixture uniformity.

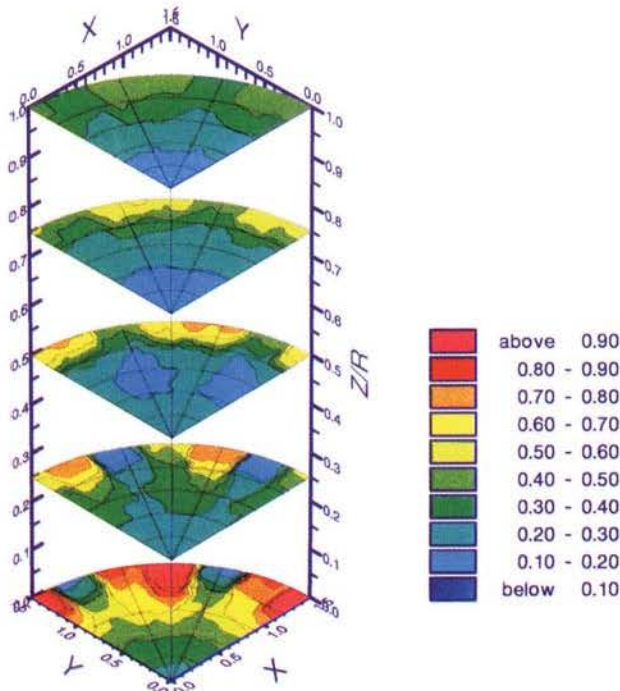


Fig. 14 Mixture fraction, *J52MOD3*, 4:1 aspect ratio slanted slots, angle = 0 deg, *J* = 51.0.

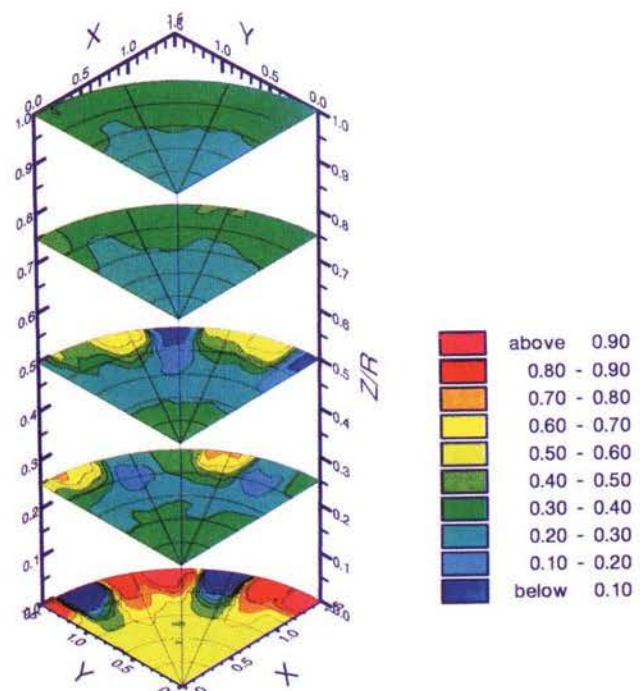


Fig. 15 Mixture fraction, *J52MOD4*, 4:1 aspect ratio slanted slots, angle = 22.5 deg, *J* = 53.0.

crossflow. For illustration, results are presented for the following four 4:1 aspect ratio modules tested at the intermediate value of *J* (52): 0 deg (*J52MOD3*), 22.5 deg (*J52MOD4*), 45 deg (*J52MOD5*), and 67.5 deg (*J52MOD6*), with respect to the mainstream direction. The mixture fraction distribution plots for these cases are shown in Figs. 14–17, respectively.

Examining the flowfield at the first axial location for these modules shows that by increasing the slot angle, the jet pen-

etration decreases. The swirl component and the circumferential mixing on the other hand improve by the increase in the slot angle.

The jet penetration at the initial axial location, although different for each module, results in similar values of the mixture uniformity parameter as shown in Fig. 18. The 0-deg slots (*J52MOD3*) produce the most jet penetration and display the worst mixture uniformity parameter at *z/R* = 1.0.

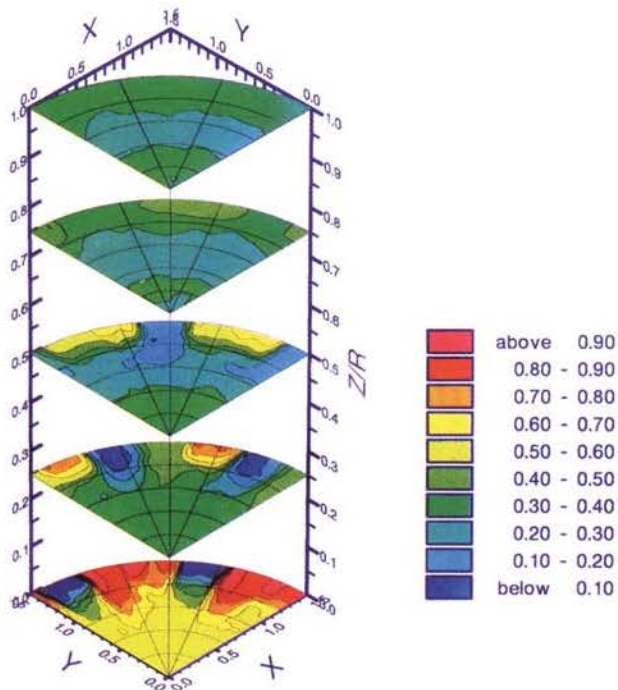


Fig. 16 Mixture fraction, *J52MOD5*, 4:1 aspect ratio slanted slots, angle = 45 deg, $J = 57.7$.

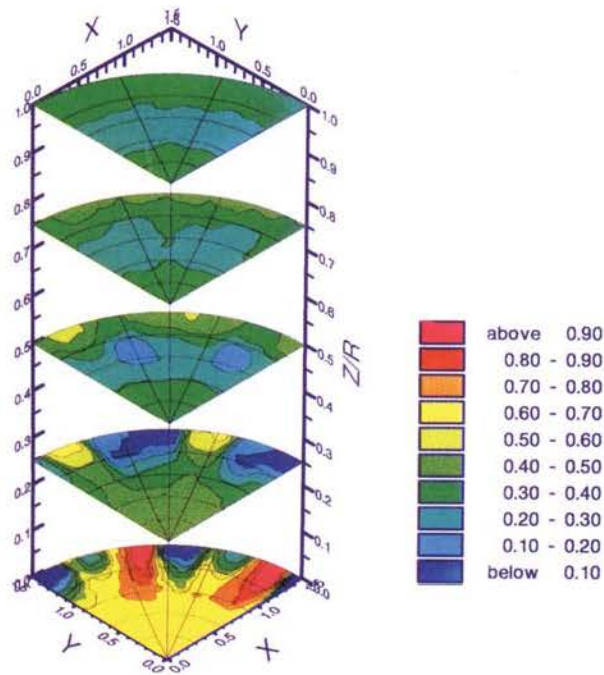


Fig. 17 Mixture fraction, *J52MOD6*, 4:1 aspect ratio slanted slots, angle = 67.5 deg, $J = 60.0$.

The other modules that impart swirl to the flow display similar values for the mixture uniformity parameter at $z/R = 1.0$. The optimum mixer based on these four cases appears to exist at an angle between 45 and 67.5 deg. These results suggest that slot angle does not have a big impact on mixture uniformity. However, this observation cannot be extended to cases where the aspect ratio, number of orifices, and momentum-flux ratio are allowed to vary along with slot angle.

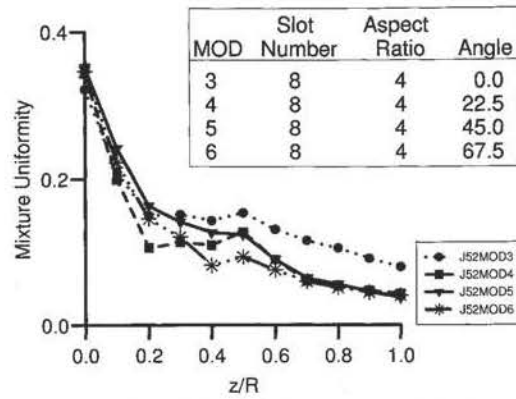


Fig. 18 Effect of slot angle on mixture uniformity.

Conclusions

- 1) Jet-to-mainstream momentum-flux ratio J , and orifice geometry significantly impact the mixing characteristics of jets in a cylindrical geometry.
- 2) For a fixed number of orifices, the coupling between J and orifice geometry determines the extent of penetration and circumferential mixing in a can configuration.
- 3) From an overall-mixing standpoint, moderate penetration to the center is desirable. Underpenetration forms a relatively unmixed core that persists at downstream locations. Overpenetration degrades circumferential mixing and forms unmixed regions along the walls.
- 4) For the momentum-flux ratio values considered, increasing the aspect ratio of slanted slots reduces jet penetration to the center and enhances mixing along the walls.
- 5) For eight 4:1 aspect ratio slot orifices at $J = 52$, increasing the angle of the slots with respect to the mainstream reduces jet penetration while not markedly affecting the mixture uniformity one duct radius from the orifice leading edge.
- 6) The near optimum mixing modules identified in this study were based on a fixed number of orifices and limited variations in orifice angle and aspect ratio. Further investigation is needed to identify optimum mixing conditions when the number of orifices, orifice aspect ratio, and angle are varied over a larger parameter space.

Acknowledgment

This work is an integral component of a program supported by the NASA Lewis Research Center, Grant NAG3-1110.

References

- ¹Shaw, R. J., "Engine Technology Challenges for a 21st Century High Speed Civil Transport," AIAA 10th International Symposium on Air Breathing Engines; also NASA TM 104363, Sept. 1991.
- ²Novick, A. S., and Troth, D. L., "Low NO_x Heavy Fuels Combustor Concept Program," Detroit Diesel Allison Div., General Motors Corp., DDA-EDR-10594; also NASA CR-165367, Oct. 1991.
- ³Smith, C. E., Talpallikar, M. V., and Holdeman, J. D., "A CFD Study of Jet Mixing in Reduced Areas for Lower Combustor Emissions," AIAA Paper 91-2460; also NASA TM 104411, June 1991.
- ⁴Talpallikar, M. V., Smith, C. E., Lai, M. C., and Holdeman, J. D., "CFD Analysis of Jet Mixing in Low NO_x Flametube Combustors," American Society of Mechanical Engineers Paper 91-GT-217; also NASA TM 104466, June 1991.
- ⁵Vranos, A., Liscinsky, D. S., True, B., and Holdeman, J. D., "Experimental Study of Cross-Stream Mixing in a Cylindrical Duct," AIAA Paper 91-2459; also NASA TM 105180, June 1991.
- ⁶Holdeman, J. D., "Mixing of Multiple Jets with a Confined Subsonic Crossflow," AIAA Paper 91-2458; also NASA TM 104412, June 1991.
- ⁷Hatch, M. S., Sowa, W. A., Samuelsen, G. S., and Holdeman, J. D., "Jet Mixing into a Heated Cross Flow in a Cylindrical Duct: Influence of Geometry and Flow Variations," AIAA Paper 92-0773; also NASA TM 105390, Jan. 1992.

⁸Kamotani, Y., and Greber, I., "Experiments on a Turbulent Jet in a Cross Flow," *AIAA Journal*, Vol. 10, No. 11, 1972, pp. 1425-1429.

⁹Fearn, R., and Weston, R. P., "Vorticity Associated with a Jet in a Cross Flow," *AIAA Journal*, Vol. 12, No. 12, 1974, pp. 1666, 1667.

¹⁰Cox, G. B., "Multiple Jet Correlation for Gas Turbine Combustor Design," *Journal of Engineering for Power*, Vol. 98, No. 2, 1976, pp. 265-273.

¹¹Holdeman, J. D., and Walker, R. E., "Mixing of a Row of Jets with a Confined Crossflow," *AIAA Journal*, Vol. 15, No. 2, 1977, pp. 243-249.

¹²Weston, R. P., and Thames, F. C., "Properties of Aspect Ratio 4.0 Rectangular Jets in a Subsonic Crossflow," *Journal of Aircraft*, Vol. 16, No. 10, 1979, pp. 701-707.

¹³Wittig, S. L. K., Elbahar, O. M. B., and Noll, B. E., "Temperature Profile Development in Turbulent Mixing of Coolant with

a Confined Hot Crossflow," *Journal of Engineering for Gas Turbines and Power*, Vol. 106, No. 1, 1984, pp. 193-197.

¹⁴Holdeman, J. D., Srinivasan, R., and Berenfeld, A., "Experiments in Dilution Jet Mixing," *AIAA Journal*, Vol. 22, No. 10, 1984, pp. 1436-1443.

¹⁵Isaac, K. M., and Jakubowski, A. K., "Experimental Study of the Interaction of Multiple Jets with a Cross Flow," *AIAA Journal*, Vol. 23, No. 11, 1985, pp. 1679-1683.

¹⁶Ho, C. M., and Gutmark, E., "Vortex Induction and Mass Entrainment in a Small-Aspect-Ratio Elliptic Jet," *Journal of Fluid Mechanics*, Vol. 179, 1987, pp. 383-405.

¹⁷Kavasaoglu, M. S., and Schetz, J. A., "Effects of Swirl and High Turbulence on a Jet in a Cross Flow," *Journal of Aircraft*, Vol. 26, No. 6, 1989, pp. 539-546.

¹⁸Stevens, S. J., and Carrotte, J. F., "Experimental Studies of Combustor Dilution Zone Aerodynamics, Part I: Mean Flowfield," *Journal of Propulsion and Power*, Vol. 6, No. 3, 1990, pp. 297-304.

Fundamentals of Aircraft Performance and Design

September 22-23, 1995 • Los Angeles, CA

Learn how to look at an aircraft and determine its mission, its performance for specified operating conditions, and the flight conditions for best performance. In addition, you will be able to perform a feasibility design to determine the general configuration of an aircraft to satisfy a specified set of operational requirements.

WHO SHOULD ATTEND

Because this course provides an overview of the relevant features of supporting technologies, (aerodynamics, propulsion, and structures), there are no prerequisites per se. Anyone interested in the performance, design, or selection of aircraft. Aerospace managers, pilots, and operational personnel, as well as anyone charged with selecting fleet aircraft or interested in buying an individual aircraft, will benefit. Anyone working directly on performance analysis or designing aircraft using computer codes will learn what is going on inside the computer, and quick and easy ways to obtain numbers that can be used to check the reasonableness and validity of computer results.

Only minimal mathematical skills are required, namely, the ability to solve quadratic equations and to differentiate and integrate. The emphasis is on simple analytical relationships and expressions that are applicable to classes of aircraft rather than on the traditional graphical techniques applied to a specific individual aircraft with a specified weight. A calculator is all you will need to solve the illustrative examples and participate in the interactive design problems.

INSTRUCTOR

Dr. Francis Joseph Hale, Professor Emeritus of Mechanical and Aerospace Engineering at North Carolina State University (NCSU).

For more information contact:

Johnnie White • Phone: 202/646-7447 • FAX: 202/646-7508



American Institute of
Aeronautics and Astronautics